

STUDYING TURBULENCE FROM DOPPLER-BROADENED ABSORPTION LINES: STATISTICS OF LOGARITHMS OF INTENSITY

A. LAZARIAN

Department of Astronomy, University of Wisconsin, Madison, US

D. POGOSYAN

Physics Department, University of Alberta, Edmonton, Canada

Draft version February 2, 2008

ABSTRACT

We continue our work on developing techniques for studying turbulence with spectroscopic data. We show that Doppler-broadened absorption spectral lines, in particularly, saturated absorption lines, can be used within the framework of the earlier-introduced technique termed the Velocity Coordinate spectrum (VCS). The VCS relates the statistics of fluctuations along the velocity coordinate to the statistics of turbulence, thus it does not require spatial coverage by sampling directions in the plane of the sky. We consider lines with different degree of absorption and show that for lines of optical depth less than one, our earlier treatment of the VCS developed for spectral emission lines is applicable, if the optical depth is used instead of intensity. This amounts to correlating the logarithms of absorbed intensities. For larger optical depths and saturated absorption lines, we show, that the amount of information that one can use is, inevitably, limited by noise. In practical terms, this means that only wings of the line are available for the analysis. In terms of the VCS formalism, this results in introducing an additional window, which size decreases with the increase of the optical depth. As a result, strongly saturated absorption lines carry the information only about the small scale turbulence. Nevertheless, the contrast of the fluctuations corresponding to the small scale turbulence increases with the increase of the optical depth, which provides advantages for studying turbulence combining lines with different optical depths. We show that, eventually, at very large optical depths the Lorentzian profile of the line gets important and extracting information on velocity turbulence, gets impossible. Combining different absorption lines one can tomography turbulence in the interstellar gas in all its complexity.

Subject headings: turbulence – ISM: general, structure – MHD – radio lines: ISM.

1. INTRODUCTION

Turbulence is a key element of the dynamics of astrophysical fluids, including those of interstellar medium (ISM), clusters of galaxies and circumstellar regions. The realization of the importance of turbulence induces sweeping changes, for instance, in the paradigm of ISM. It became clear, for instance, that turbulence affects substantially star formation, mixing of gas, transfer of heat. Observationally it is known that the ISM is turbulent on scales ranging from AUs to kpc (see Armstrong et al 1995, Elmegreen & Scalo 2004), with an embedded magnetic field that influences almost all of its properties.

The issue of quantitative descriptors that can characterize turbulence is not a trivial one (see discussion in Lazarian 1999 and ref. therein). One of the most widely used measures is the turbulence spectrum, which describes the distribution of turbulent fluctuations over scales. For instance, the famous Kolmogorov model of incompressible turbulence predicts that the difference in velocities at different points in turbulent fluid increases on average with the separation between points as a cubic root of the separation, i.e. $|\delta v| \sim l^{1/3}$. In terms of direction-averaged energy spectrum this gives the famous Kolmogorov scaling $E(k) \sim 4\pi k^2 P(\mathbf{k}) \sim k^{5/3}$, where $P(\mathbf{k})$ is a 3D energy spectrum defined as the Fourier transform of the correlation function of velocity fluctuations $\xi(\mathbf{r}) = \langle \delta v(\mathbf{x})\delta v(\mathbf{x} + \mathbf{r}) \rangle$. Note that in this paper we use $\langle \dots \rangle$ to denote averaging procedure.

Quantitative measures of turbulence, in particular, turbulence spectrum, became important recently also due to advances in the theory of MHD turbulence. As we know, astrophysical fluids are magnetized, which makes one believe that the correspondence should exist between astrophysical turbulence and MHD models of the phenomenon (see Vazquez-Semadeni et al. 2000, Mac Low & Klessen 2004, Bellesteros-Paredes et al. 2007, McKee & Ostriker 2007 and ref. therein).

In fact, without observational testing, the application of theory of MHD turbulence to astrophysics could always be suspect. Indeed, from the point of view of fluid mechanics astrophysical turbulence is characterized by huge Reynolds numbers, Re , which is the inverse ratio of the eddy turnover time of a parcel of gas to the time required for viscous forces to slow it appreciably. For $Re \gg 100$ we expect gas to be turbulent and this is exactly what we observe in HI (for HI $Re \sim 10^8$). In fact, very high astrophysical Re and its magnetic counterpart magnetic Reynolds number Rm (that can be as high as $Rm \sim 10^{16}$) present a big problem for numerical simulations that cannot possibly get even close to the astrophysically-motivated numbers. The currently available 3D simulations can have Re and Rm up to

$\sim 10^4$. Both scale as the size of the box to the first power, while the computational effort increases as the fourth power (3 coordinates + time), so the brute force approach cannot begin to resolve the controversies related, for example, to ISM turbulence.

We expect that observational studies of turbulence velocity spectra will provide important insights into ISM physics. Even in the case of much more simple oceanic (essentially incompressible) turbulence, studies of spectra allowed to identify meaningful energy injection scales. In interstellar, intra-cluster medium, in addition to that, we expect to see variations of the spectral index arising from the variations of the degree of compressibility, magnetization, interaction of different interstellar phases etc.

How to get the turbulence spectra from observations is a problem of a long standing. While density fluctuations are readily available through both interstellar scintillations and studies of column density maps, the more coveted velocity spectra have been difficult to obtain reliably until very recently.

Turbulence is associated with fluctuating velocities that cause fluctuations in the Doppler shifts of emission and absorption lines. Observations provide integrals of either emissivities or opacities, both proportional to the local densities, at each velocity along the line of sight. It is far from trivial to determine the properties of the underlying turbulence from the observed spectral line.

Centroids of velocity (Munch 1958) have been an accepted way of studying turbulence, although it was not clear to when and to what extend the measure really represents the velocity. Recent studies (Lazarian & Esquivel 2003, henceforth LE03, Esquivel & Lazarian 2005, Ossenkopf et al 2006, Esquivel et al. 2007) have showed that the centroids are not a good measure for supersonic turbulence, which means that while the results obtained for HII regions (O'Dell & Castaneda 1987) are probably OK, those for molecular clouds are unreliable.

An important progress in analytical description of the relation between the spectra of turbulent velocities and the observable spectra of fluctuations of spectral intensity was obtained in Lazarian & Pogosyan (2000, henceforth LP00). This description paved way to two new techniques, which were later termed Velocity Channel Analysis (VCA) and Velocity Coordinate Spectrum (VCS).

The techniques provide different ways of treating observational data in Position-Position-Velocity (PPV) data cubes. While VCA is based on the analysis of channel maps, which are the velocity slices of PPV cubes, the VCS analyses fluctuations along the velocity direction. If the slices have been used earlier for turbulence studies, although the relation between the spectrum of intensity fluctuations in the channel maps and the underlying turbulence spectrum was unknown, the analysis of the fluctuations along the velocity coordinate was initiated by the advent of the VCS theory.

With the VCA and the VCS one can relate both observations and simulations to *turbulence theory*. For instance, the aforementioned turbulence indexes are very informative, e.g. velocity indexes steeper than the Kolmogorov value of $-5/3$ are likely to reflect formation of shocks, while shallower indexes may reflect scale-dependent suppression of cascading (see Beresnyak & Lazarian 2006 and ref. therein). By associating the variations of the index with different regions of ISM, e.g. with high or low star formation, one can get an important insight in the fundamental properties of ISM turbulence, its origin, evolution and dissipation.

The absorption of the emitted radiation was a concern of the observational studies of turbulence from the very start of the work in the field (see discussion in Munch 1999). A quantitative study of the effects of the absorption was performed for the VCA in Lazarian & Pogosyan (2004, henceforth LP04) and for the VCS in Lazarian & Pogosyan (2006, henceforth LP06). In LP06 it was stressed that absorption lines themselves can be used to study turbulence. Indeed, the VCS is a unique technique that does not require a spatial coverage to study fluctuations. Therefore individual point sources sampling turbulent absorbing medium can be used to get the underlying turbulent spectra.

However, LP06 discusses only the linear regime of absorption, i.e. when the absorption lines are not saturated. This substantially limits the applicability of the technique. For instance, for many optical and UV absorption lines, e.g. Mg II, SiII, SiIII the measured spectra show saturation. This means that a part of the wealth of the unique data obtained e.g. by HST and other instruments cannot be handled with the LP06 technique.

The goal of this paper is to improve this situation. In particular, in what follows, we develop a theoretical description that allows to relate the fluctuations of the absorption line profiles and the underlying velocity spectra in the saturated regime.

Below, in §2 we describe the setting of the problem we address, while our main derivations are in §3. The discussion of the new technique of turbulence study is provided in §4, while the summary is in §5.

2. ABSORPTION LINES AND MATHEMATICAL SETTING

While in our earlier publications (LP00, LP04, LP06) concentrated on emission line, in particular radio emission lines, e.g. HI and CO, absorption lines present the researchers with well defined advantages. For instance, they allow to test turbulence with a pencil beam, suffer less from uncertainties in path length. In fact, studies of absorption features in the spectra of stars have proven useful in outlining the gross features of gas kinematics in Milky way. Recent advances in sensitivity and spectral resolution of spectrographs allow studies of turbulent motions.

Among the available techniques, VCS is the leading candidate to be used with absorption lines. Indeed, it is only with extended sources that the either centroid or VCA studies are possible. At the same time, VCS makes use not of the spatial, but frequency resolution. Thus, potentially, turbulence studies are possible if absorption along a single line is available. In reality, information along a few lines of sight, as it shown in Fig 1 is required to improve the statistical accuracy of the measured spectrum. Using the simulated data sets Chepurnov & Lazarian (2006ab) experimentally established that the acceptable number of lines ranges from 5 to 10.

For weak absorption, the absorption and emission lines can be analyzed in the same way, namely, the way suggested in LP06. For this case, the statistics to analyse is the squared Fourier transform of the Doppler-shifted spectral line, irrespectively of the fact whether this is an emission or an absorption spectral line. Such a “spectrum of spectrum” is not applicable for saturated spectral lines, which width is still determined by the Doppler broadening. It is known (see Spitzer 1978) that this regime corresponds to the optical depth τ ranging from 10 to 10^3 . The present paper will concentrate on this regime¹.

Observations in absorption line

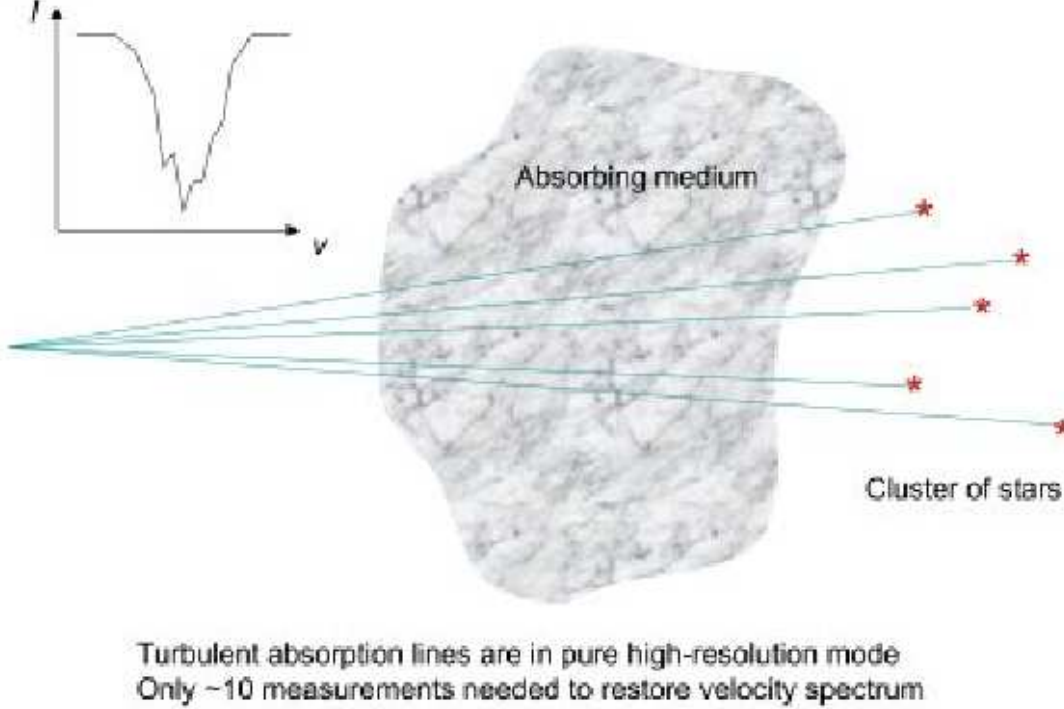


FIG. 1.— Absorption line study of turbulence in a cloud with VCS.

Consider the problem in a more formal way. Intensity of the absorption line at frequency ν is given as

$$I(\nu, \nu_0) = I_0 e^{-\tau(\nu, \nu_0)} \quad (1)$$

where $\tau(\nu)$ is the optical depth. In the limit of vanishing intrinsic width of the line $\phi_i(\nu - \nu_0) = \alpha\delta(\nu - \nu_0)$, the frequency spread of $\tau(\nu, \nu_0)$ is determined solely by the Doppler shift of the absorption frequency from moving atoms.

The number density of atoms along the line of sight moving at required velocity $v \approx \frac{c}{\nu_0}(\nu - \nu_0)$ is

$$\rho_s(v) = \int_0^S dz \rho(z) \phi(v - u(z) - v_{reg}) \quad (2)$$

where ϕ is the thermal distribution centered at every point z at the local mean velocity that is determined by the sum of turbulent and regular flow at that point. This is the density in PPV coordinate that we introduced in LP00, so $\tau(\nu) = \alpha(\nu_0)\rho_s(v)$. The intrinsic line width is accounted for by the convolution

$$\tau(v) = \alpha(\nu_0) \int dw \rho_s(w) \phi_i(w - v) \quad (3)$$

or, in more detail,

$$\tau(v) = \alpha(\nu_0) \int_0^S dz n(z) \int dw \phi(w - u(z) - v_{gal}(z)) \phi_i(w - v) . \quad (4)$$

With intrinsic profile given by the Lorenz form $\phi_i(w - v) = \frac{a/\pi}{(w-v)^2 + a^2}$, the inner integral gives the shifted Voigt profile

$$H(v - u(x) - v_{gal}(x)) = \frac{1}{\pi\sqrt{2\beta}} \int dw \frac{a}{(w - v)^2 + a^2} \exp\left(-\frac{(w - u(x) - v_{gal}(x))^2}{2\beta}\right) , \quad (5)$$

¹ It is known that for τ larger than 10^5 the line width is determined by atomic constants and therefore it does not carry information about turbulence.

so we have another representation

$$\tau(v) = \alpha(\nu_0) \int_0^S dz n(x) H(v - u(x)) . \quad (6)$$

We clearly see from Eq. (6) that the line is affected both by Doppler shifts² and atomic constants.

3. FLUCTUATIONS OF OPTICAL DEPTH

3.1. Statistics of Optical Depth Fluctuations

The optical depth as a function of frequency contains fluctuating component arising from turbulent motions and associated density inhomogeneities of the absorbers. Statistics of optical depth fluctuations along the line of sight therefore carries information about turbulence in ISM.

The optical depth is determined by the density of the absorbers in the PPV space, ρ_s . In our previous work we have studied statistical properties of ρ_s in the context of emission lines, using both structure function and power spectrum formalisms. Absorption lines demonstrate several important differences that warrant separate study.

Firstly, our ability to recover the optical depth from the observed intensity

$$I(\nu) = I_0 e^{-\tau(\nu)} + N \quad (7)$$

depends on the magnitude of the absorption as well as sensitivity of the instrument and the level of measurement noise N .

For lines with low optical depth $\tau_0 < -\ln(N/I_0)$ we can in principle measure the optical depth throughout the whole line. At higher optical depths, the central part of the line is saturated below the noise level and the useful information is restricted to the wings of the line. This is the new regime that is the subject of this paper.

In this regime the data is available over a window of frequencies limited to velocities high enough so that $\tau(v) < -\ln(N/I_0)$ but not as high as to have Lorentz tail define the line. Higher the overall optical depth, narrower are the wings (following Spitzer, at $\tau_0 > 10^5$ the wings are totally dominated by Lorentz factor). We shall denote this window by $W(v - v_0, \Delta)$ where v_0 is the velocity that the window is centered upon (describing frequency position of the wing) and Δ is the wing width. It acts as a mask on the “underlying” data

$$\tau(v) \rightarrow \tau(v) W(v - v_0, \Delta) . \quad (8)$$

Secondly, fluctuations in the wings of a line are superimposed on the frequency dependent wing profile. In other words, the statistical properties of the optical depth are inhomogeneous in this frequency range, with frequency dependent statistical mean value. While *fluctuations* of the optical depth $\delta\tau(v)$ that have origin in the turbulence can still be assumed to be statistically homogeneous, the mean profile of a wing must be accounted for.

What statistical descriptors one should chose in case of line of sight velocity data given over limited window? Primary descriptors of a random field, here $\tau(v)$, are the ensemble average product of the values of the field at separated points — the two point correlation function

$$\xi_\tau(v_1, v_2) = \langle \tau(v_1) \tau(v_2) \rangle \quad (9)$$

and, reciprocally, the average square of the amplitudes of its (Fourier) harmonics decomposition — the power spectrum

$$P_\tau(k_{v,1} k_{v,2}) = \langle \tau(k_{v,1}) \tau^*(k_{v,2}) \rangle \quad (10)$$

In practice these quantities are measurable if one can replace ensemble average by averaging over different positions which relies on some homogeneity properties of stochastic process. We assume that underlying turbulence is homogeneous and isotropic. This does not make the optical depth to be statistically homogeneous in the wings of the line, but allows to introduce the fluctuations of τ on the background of the mean profile $\bar{\tau}(v)$, $\Delta\tau(v) = \tau(v) - \bar{\tau}(v)$, which are (LP04)

$$\xi_{\Delta\tau}(v) = \langle \Delta\tau(v_1) \Delta\tau(v_2) \rangle , \quad v = v_1 - v_2 \quad (11)$$

$$P_{\Delta\tau}(k_{v,1} k_{v,2}) = \langle \Delta\tau(k_{v,1}) \Delta\tau^*(k_{v,2}) \rangle \delta(k_{v,1} - k_{v,2}) \quad (12)$$

Homogeneous correlation function depends only on a point separation and amplitudes of distinct Fourier harmonics are independent. The obvious relations are

$$\xi_\tau(v_1, v_2) = \xi_{\Delta\tau}(v) + \bar{\tau}(v_1) \bar{\tau}(v_2) \quad (13)$$

$$P_\tau(k_{v,1} k_{v,2}) = P_{\Delta\tau}(k_v) + \bar{\tau}(k_{v,1}) \bar{\tau}^*(k_{v,2}) \quad (14)$$

Although mathematically the power spectrum is just a Fourier transform of the correlation function

$$P_{\Delta\tau}(k_v) = \int e^{ik_v v} \xi_{\Delta\tau}(v) dv , \quad (15)$$

which of them is best estimated from data depends on the properties of the signal and the data.

² Speaking formally, one can always make use of the known atomic constants and get inside into turbulence. This is not practical, however, for an actual spectrum in the presence of noise.

The power spectrum carries information which is localized to a particular scale and as such is insensitive to processes that contribute outside the range of scales of interest, in particular to long-range smooth variations. On the other hand, determination of Fourier harmonics is non-local in configuration space and is sensitive to specifics of data sampling – the finite window, discretization, that all lead to aliasing of power from one scales to another. The issue is severe if the aliased power is large.

Conversely, the correlation function is localized in configuration space and can be measured for non-uniformly sampled data. However, at each separation it contains contribution from all scales and may mix together the physical effects from different scales. In particular, $\xi(v)$ is not even defined for power law spectra $P(k_v) \sim k_v^{-n}$ with index $n \geq 1$ (for one dimensional data)³. This limitation is relieved if one uses the structure function

$$D_{\Delta\tau}(v) = \langle (\Delta\tau(v_1) - \Delta\tau(v_2))^2 \rangle \quad (16)$$

instead, which is well defined for $n < 3$. The structure function can be thought of as regularized version of the correlation function

$$D_{\Delta\tau}(v) = 2(\xi_{\Delta\tau}(0) - \xi_{\Delta\tau}(v)) \quad (17)$$

that is related to the power spectrum in the same way as the correlation function, if one excludes the $k_v = 0$ mode.

Velocity Coordinate Spectrum studies of LP06 demonstrated that the expected one dimensional spectrum of PPV density fluctuations along velocity coordinate that arise from turbulent motions is $P(k_v) \sim k_v^{-2/m}$ where m is the index of line-of-sight component of the velocity structure function. For Kolmogorov turbulence $m = 2/3$ and for turbulent motions dominated by shocks $m = 1/2$. These spectra are steep $\sim k_v^{-3}, \sim k_v^{-4}$ which makes the direct measurement of the structure functions impractical (although for $m > 2/3$ the structure function can be defined). At the same time, in our present studies we deal with a limited range of data in the wings of the absorption lines, which complicates the direct measurements of the power spectrum.

Below we first describe the properties of the power spectrum $P_{\Delta\tau}(k_v)$ in this case, and next develop the formalism of higher order structure functions.

3.2. Power Spectrum of Optical Depth Fluctuations

Let us derive the power spectrum of the optical depth fluctuations, $P_\tau(k_v) \equiv \langle \tau(k_v)\tau^*(k_v) \rangle$ Here k_v is wave number reciprocal to the velocity (frequency) separation between two points on the line-of-sight and angular brackets denote an ensemble averaging.⁴

Fourier transform of the eq. (6) with respect to velocity is

$$\tau(k_v) = \alpha(\nu_0) \int_0^S dz n(x) \int dk'_v e^{-|k'_v|a} e^{-\frac{k'^2\beta}{2}} e^{-ik'_v u(x)} W(k_v - k'_v, v_0, \Delta) \quad (18)$$

and the power spectrum

$$P_\tau(k_v) = \left\langle \alpha(\nu_0)^2 \int_0^S dz_1 \int_0^S dz_2 n(z_1)n(z_2) \times \right. \\ \left. \int dk'_v \int dk''_v e^{-(|k'_v|+|k''_v|)a} e^{-\frac{(k'^2+k''^2)\beta}{2}} e^{-i[k'_v u(z_1)-k''_v u(z_2)]} W(k_v - k'_v) W^*(k_v - k''_v) \right\rangle \quad (19)$$

which is useful to express using average velocity $u_+ = (u(z_1) + u(z_2))/2$ and velocity difference $u = u(z_1) - u(z_2)$, as well as correspondent variables for the wave numbers $k_v^+ = (k'_v + k''_v)/2$ and $k_v^- = k'_v - k''_v$, as

$$P_\tau(k_v) = \left\langle \alpha(\nu_0)^2 \int_0^S dz_1 \int_0^S dz_2 n(z_1)n(z_2) \int_{-\infty}^{\infty} dk_v^+ e^{-k_v^+{}^2\beta} e^{ik_v^+ u} \right. \\ \left. \times \int_{-\infty}^{\infty} dk_v^- e^{-\frac{1}{4}k_v^-{}^2\beta} e^{ik_v^- u_+} e^{-(|k_v^+|+|k_v^-|)a} W\left(k_v - k_v^+ - \frac{k_v^-}{2}\right) W^*\left(k_v - k_v^+ + \frac{k_v^-}{2}\right) \right\rangle \quad (20)$$

The fluctuating, random quantities, over which the averaging is performed are the density $n(z)$ and the line-of-sight component of the velocity of the absorbers $u(z)$, varying along the line of sight . In our earlier papers (see LP00, LP04) we argued that in many important cases they can be considered as uncorrelated between themselves, so that

$$\langle n(z_1)n(z_2)e^{ik_v^+ u} e^{ik_v^- u_+} \rangle = \xi(|z_1 - z_2|) e^{-\frac{1}{2}k_v^+{}^2 D_z(|z_1 - z_2|)} e^{-\frac{1}{4}k_v^-{}^2 [D_z(S) - D_z(|z_1 - z_2|)/2]} , \quad (21)$$

where $\xi(|z_1 - z_2|)$ is the correlation function of the density of the absorbers and $D_z(|z_1 - z_2|)$ is the structure function of their line-of-sight velocity due to turbulent motions. D_z is expected to saturate at the value $D_s(S)$ for separations

³ In physically realistic situations the power law will not, of course, extend infinitely to large scales. Mathematical divergence of the correlation function in practice mean that for steep spectra the largest present scales the correlation at all, even small separations v .

⁴ note, that due to having measurements in the finite window, the amplitudes at different waves numbers are, in general, correlated, $\langle \tau(k_v)\tau^*(k'_v) \rangle \neq 0$, $k_v \neq k'_v$. Here we restrict ourselves to diagonal terms only.

of the size of the absorbing cloud S . The dependence of $\xi(z)$ and $D_z(z)$ only on spatial separation between a pair of absorbers reflects the assumed statistical homogeneity of the turbulence model. Introducing $z = z_1 - z_2$ and performing integration over $z_+ = (z_1 + z_2)/2$ one obtains⁵

$$\begin{aligned} P_\tau(k_v) &= \alpha^2 S \int_0^S dz(S - |z|) \xi(z) \int_0^\infty dk_v^+ e^{-2k_v^+ a} e^{-\frac{1}{2} k_v^{+2} D^-} \int_0^\infty dk_v^- e^{-\frac{1}{4} k_v^{-2} D^+} \tilde{W}\left(k_v, k_v^+, \frac{k_v^-}{2}\right) \\ &\quad + \text{correction terms (see Appendix)} \end{aligned} \quad (22)$$

where $D^- = D_z(|z_1 - z_2|) + 2\beta$, $D^+ = D_z(S) - D_z(|z_1 - z_2|)/2 + \beta$ and symmetrized window \tilde{W} is defined in the Appendix.

If one has the whole line available for analysis, the masking window will be flat with $\delta(k)$ -function like Fourier transform. The combination of the windows in the power spectrum will translate to $\delta(k_v - k_v^+) \delta(k_v^-)$ and

$$P_\tau(k_v) \sim 2\alpha(\nu_0)^2 S e^{-2k_v a - k_v^{+2} \beta} \int_0^S dz(S - |z|) \xi(z) e^{-\frac{1}{2} k_v^{+2} D^-} \quad (23)$$

Masking the data has the effect of aliasing modes of the large scales that exceed the available data range, to shorter wavelength. This is represented by the convolution with Fourier image of the mask. Secondary effect is the contribution of the modes with different wave numbers $k_v^- \neq 0$ to the diagonal part of the power spectrum. This again reflects the situation that different Fourier components are correlated in the presence of the mask.

To illustrate the effects of the mask, let us assume that we select the line wing with the help of a Gaussian mask centered in the middle of the wing at v_1

$$W(v - v_1, \Delta) = e^{-\frac{(v-v_1)^2}{2\Delta^2}} \quad (24)$$

$$W(k_v) = \sqrt{2\pi} \Delta e^{-ik_v v_1} e^{-\frac{1}{2} k_v^2 \Delta^2} \quad (25)$$

that gives

$$\tilde{W} = 4\pi \Delta^2 \cos\left(\frac{k_v^-}{2} v_1\right) e^{-\frac{k_v^{-2} \Delta^2}{4}} \left(e^{-(k_v - k_v^+)^2 \Delta^2} + e^{-(k_v + k_v^+)^2 \Delta^2} \right) \quad (26)$$

All integrals can then be carried out to obtain

$$\begin{aligned} P(k_v) &\sim \alpha^2 S \int_0^S dz(S - z) \xi(z) \frac{\Delta^2 \exp\left[-\frac{1}{4} \frac{v_1^2}{D^+ + \Delta^2}\right]}{\sqrt{(D^+ + 2\Delta^2)(D^- + 2\Delta^2)}} \exp\left[-\frac{\Delta^2 D^-}{D^- + 2\Delta^2} k_v^2\right] \\ &\quad \times \exp\left[\frac{2a^2}{D^- + 2\Delta^2}\right] \left\{ \exp\left[\frac{-4a\Delta^2 k_v}{D^- + 2\Delta^2}\right] \operatorname{Erfc}\left[\frac{\sqrt{2}(a - \Delta^2 k_v)}{\sqrt{D^- + 2\Delta^2}}\right] + (k_v \rightarrow -k_v) \right\} \end{aligned} \quad (27)$$

The following limits (taking $k_v > 0$) are notable:

$$\Delta \rightarrow \infty : \quad (28)$$

$$P(k_v) \propto \alpha(\nu_0)^2 S \int_0^S dz(S - z) \xi(z) \exp\left[-\frac{1}{2} k_v^2 D^- - 2ak_v\right] \quad a \rightarrow 0 : \quad (29)$$

$$P(k_v) \propto \alpha(\nu_0)^2 S \int_0^S dz(S - z) \xi(z) \frac{\Delta^2 \exp\left[-\frac{1}{4} \frac{v_1^2}{D^+ + \Delta^2}\right]}{\sqrt{(D^+ + 2\Delta^2)(D^- + 2\Delta^2)}} \exp\left[-\frac{\Delta^2 D^-}{D^- + 2\Delta^2} k_v^2\right]$$

The last expression particularly clearly demonstrates the effect of the window, which width in case of the line wing is necessarily limited by $\Delta^2 < D(S) + 2\beta$. The power spectrum is corrupted at scales $k_v < \Delta^{-1}$, but still maintains information about turbulence statistics for $k_v \gg \Delta^{-1}$. Indeed, in our integral representation the power spectrum at k_v is determined by the linear scales such that $\frac{\Delta^2 D^-}{D^- + 2\Delta^2} k_v^2 < 1$ which translates into $D^- < 2\Delta^2/(k_v^2 \Delta^2 - 1)$. Thus, if $k_v \Delta \gg 1$ over all scales defining power at k_v one has $\Delta \gg D^-$ and there is no significant power aliasing.⁶ For intermediate scales there is a power aliasing as numerical results demonstrate in Figure 2. Doppler broadening described by D^- incorporates both turbulent and thermal effects. Thermal effects are especially important in case of narrow line wings, since the range of the wavenumbers relatively unaffected by both thermal motions and the mask is limited $1/\sqrt{\beta} > k_v > \Delta^{-1}$ and exists only for relatively wide wings $\Delta > \sqrt{\beta}$. For narrower wings the combined turbulent and thermal profile must be fitted to the data, possibly determining the temperature of the absorbers at

⁵ Absolute values in the Fourier image of the Lorentz transform require separate consideration of each quadrant of wave numbers. This is carried out in the Appendix.

⁶ In this regime the first factor is essentially constant since $D^+(z) = D_z(S) + 2\beta - D^-(z)/2$ varies little, $D^+(z) \approx D^+(0)$ in the interval $2\beta < D^- < 2k_v^{-2} \ll 2\Delta^2 < D(S) + 2\beta$.

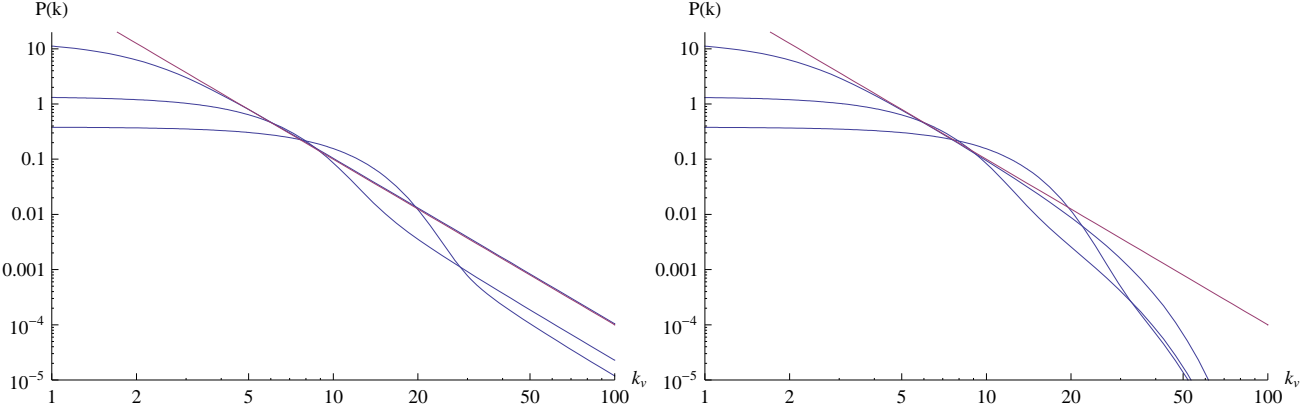


FIG. 2.— Power spectrum of the optical depth fluctuations from line wings. All parameters, k_v , Δ , $\sqrt{\beta}$, v_1 are dimensionless, in the units of $\sqrt{D_z(S)}$, the variance of the turbulent velocity at the scale of the cloud. Intrinsic line broadening is neglected. Only the effect of the turbulent motions and not spatial inhomogeneity of the absorbers is taken into account. The underlying scaling of the turbulent velocities is Kolmogorov, $m = 2/3$. The left panel illustrates the power aliasing due to finite width of the window. The power spectrum is plotted, from top to bottom, for $\Delta = 1, 0.2, 0.1$, i.e. the widths of the wing ranges from the complete line to one-tenth of the line width. The straight line shows the power law $P(k_v) \propto k_v^{-2/m} = k_v^{-3}$ expected under ideal observational circumstances. One finds that for the ideal Gaussian mask the underlying spectrum is recovered for $k_v > 3\Delta^{-1}$. The right panel shows the modification of the spectrum due to thermal broadening, which is taken at the level $\sqrt{\beta} = \frac{1}{30}\sqrt{D_z(S)}$. Thermal effects must be accounted for for $k_v > 1/(3\sqrt{\beta})$.

the same time. This recipe is limited by the assumption that the temperature of the gas is relatively constant for the absorbers of a given type.

We should note that the Gaussian window provides one of the ideal cases, limiting the extend of power aliasing since the window Fourier image falls off quickly. One of the worst scenarios is represented by sharp top hat mask, which Fourier image falls off only as k_v^{-2} spreading the power from large scales further into short scales. For steep spectra that we have in VCS studies all scales may experience some aliasing. This argues for extra care while treating the line wings through power spectrum or for use of alternative approaches.

3.3. Second order structure function

Second order structure function provides an alternative to power spectrum measurement in case of steep spectra with the data limited to the section of the lines. The second order structure function of the fluctuations of the optical depth can be defined as

$$dD_{\Delta\tau}(v) = \frac{1}{2} \left\langle (\Delta\tau(v_1 + v) + \Delta\tau(v_1 - v) - 2\Delta\tau(v_1))^2 \right\rangle \quad (30)$$

It represents additional regularization of the correlation function beyond the ordinary structure function

$$dD_{\Delta\tau}(v) = 3\xi_{\Delta\tau}(0) - 4\xi_{\Delta\tau}(v) + \xi_{\Delta\tau}(2v) \quad (31)$$

$$= 2D_{\Delta\tau}(v) - \frac{1}{2}D_{\Delta\tau}(2v) \quad (32)$$

$D_{\Delta\tau}(v)$ is proportional to three dimensional velocity space density structure function at zero angular separations $d_\rho(0, v)$, discussed in LP06. Using the results of LP06 for $d_\rho(0, v)$ we obtain

$$\begin{aligned} dD_{\Delta\tau}(v) &\sim \left(\frac{r_0}{S}\right)^\gamma \int_{-1}^1 dz \frac{1}{|\hat{z}|^{\gamma+m/2}} \left[3 - 4 \exp\left(-\frac{\hat{v}^2}{2|\hat{z}|^m}\right) + \exp\left(-\frac{2\hat{v}^2}{|\hat{z}|^m}\right) \right] \\ &\propto \frac{\bar{\rho}^2 S^2}{D_z(S)} \frac{1}{m} \left(\frac{r_0}{S}\right)^\gamma \left[\hat{v}^{2p} \Gamma(-p) (2^{p-1} - 2^{1-p}) + \frac{2^{4p-6}}{p-2} \hat{v}^4 + O(\hat{v}^6) \right] \end{aligned} \quad (33)$$

where $p = (1 - \gamma)/m - 1/2 > 0$ and γ is the correlation index that describes spatial inhomogeneities of the absorbers. To shorten intermediate formulas, the dimensionless quantities $\hat{v} = v/D_z^{1/2}(S)$, $\hat{z} = z/S$, $\hat{r} = r/S$ are introduced. The first term in the expansion contains information about the underlying field, while the power law series represent the effect of boundary conditions at the cloud scale. In contrast to ordinary correlation function they are not dominant until $p \geq 2$, i.e. for $(1 - \gamma)/m < 5/2$ the second order structure function is well defined. When turbulent motions provide the dominant contribution to optical depth fluctuations, $\gamma = 0$, we see that measuring the dD_{τ} one can recover the turbulence scaling index if $m > 2/5$, which includes both interesting cases of Kolmogorov turbulence and shock-dominated motions. This condition is replaced by $m > 2/5(1 - \gamma)$ if the density fluctuations, described by correlation index γ , are dominant.

At sufficiently small scales the second order structure function has the same scaling as the first order one

$$dD_{\Delta\tau}(v) \propto \frac{\bar{\rho}^2 S^2}{D_z(S)} \frac{1}{m} \left(\frac{r_0}{S}\right)^\gamma (2^{p-1} - 2^{1-p}) \Gamma(-p) \cdot \hat{v}^{2p} \quad (34)$$

A practical issue of measuring the structure functions directly in the wing of the line is to take into account the line profile. The directly accessible

$$dD_\tau(v_1, v) = \frac{1}{2} \left\langle (\tau(v_1 + v) + \tau(v_1 - v) - 2\tau(v_1))^2 \right\rangle \quad (35)$$

is related to the structure function of the fluctuations as

$$dD_{\Delta\tau}(v) = dD_\tau(v_1, v) - \frac{1}{2} (\bar{\tau}(v_1 + v) + \bar{\tau}(v_1 - v) - 2\bar{\tau}(v_1))^2 \quad (36)$$

where the mean profile of the optical depth $\bar{\tau}$ is related to the mean profile of PPV density $\bar{\rho}_s$ given in the Appendix B of LP06. At small separations v , the correction to the structure function due to mean profile behaves as v^4 and is subdominant.

The price one pays when utilizing higher-level structure function is their higher sensitivity to the noise in the data. While correlation function itself is not biased by the noise except at zero separations (assuming noise is uncorrelated

$$\langle [\tau(v_1) + N(v_1)][\tau(v_1 + v) + N(v_1 + v)] \rangle = \xi_\tau(v) + \langle N^2 \rangle \delta(v) \quad (37)$$

already the structure function is biased by the noise which contributes to all separations

$$\langle [\tau(v_1) + N(v_1) - \tau(v_1 + v) - N(v_1 + v)]^2 \rangle = D_\tau(v) + 2\langle N^2 \rangle \quad (38)$$

This effect is further amplified for the second order structure function

$$\frac{1}{2} \left\langle [\tau(v_1 + v) + \tau(v_1 - v) - 2\tau(v_1) + N(v_1 + v) + N(v_1 - v) - 2N(v_1)]^2 \right\rangle = dD_\tau(v) + 3\langle N^2 \rangle \quad (39)$$

The error in the determination of the structures function of higher order due to noise also increases.

3.4. Comparison of the approaches

Structure functions and power spectra are used interchangeably in the theory of turbulence (see Monin & Yaglom 1975). However, complications arise when spectra are "extremely steep", i.e. the corresponding structure function of fluctuation grows as x^\aleph , $\aleph > 2$. For such random fields, one cannot use ordinary structure functions, while the one dimensional Fourier transforms that is employed in VCS corresponds to the power spectrum of $k_v^{-1-\aleph}$ is well defined.

As a rule, one does not have to deal with so steep spectra in theory of turbulence (see, however, Cho et al. 2002 and Cho & Lazarian 2004). Within the VCS, such "extremely steep" spectra emerge naturally, even when the turbulence is close to being Kolmogorov. This was noted in LP06, where the spectral approach was presented as the correct one to studying turbulence using fluctuations of intensity along v-coordinate.

The disadvantage of the spectral approach is when the data is being limited by a non-Gaussian window function. Then the contributions from the scales determined by the window function may interfere in the obtained spectrum at large k_v . An introduction of an additional more narrow Gaussian window function may mitigate the effect, but limits the range of k_v for which turbulence can be studied. Thus, higher order structure functions (see the subsection above), is advantageous for the practical data handling.

In terms of the VCA theory, we used mostly spectral description in LP00, while in LP04, dealing with absorption, we found advantageous to deal with real rather than Fourier space. In doing so, however, we faced the steepness of the spectrum along the v-coordinate and provided a transition to the Fourier description to avoid the problems with the "extremely steep" spectrum. Naturally, our approach of higher order structure functions is applicable to dealing with the absorption within the VCA technique.

4. DISCUSSION

4.1. Simplifying assumptions

In the paper above we have discussed the application of VCS to strong absorption lines. The following assumption were used. First of all, considering the radiative transfer we neglected the effects of stimulated emission. This assumption is well satisfied for optical or UV absorption lines (see Spitzer 1979). Then, we assumed that the radiation is coming from a point source, which is an excellent approximation for the absorption of light of a star or a quasar. Moreover, we disregarded the variations of temperature in the medium.

Within our approach the last assumption may be most questionable. Indeed, it is known that the variations of temperature do affect absorption lines. Nevertheless, our present study, as well as our earlier studies, prove that the effects of the variations of density are limited. It is easy to see that the temperature variations can be combined together with the density ones to get effective renormalized "density" which effects we have already quantified.

Our formalism can also be generalized to include a more sophisticated radiative transfer and the spatial extend of the radiation source. In the latter case we shall have to consider both the case of a narrow and a broad telescope beam, the way it has been done in LP06. Naturally, the expressions in LP06 for a broad beam observations can be straightforwardly applied to the absorption lines, substituting the optical depth variations instead of intensities. The advantage of the extended source is that not only VCS, but also VCA can be used (see Deshpande et al. 2000). As a disadvantage of an extended source is the steepening of the observed v-coordinate spectrum for studies of unresolved turbulence. This, for instance, may require employing even higher order structure functions, if one has to deal with windows arising from saturation of the absorption line.

In LP06 we have studied the VCS technique in the presence of absorption and formulated the criterion for the fluctuations of intensity to reliably reflect the fluctuations in turbulent velocities. In this paper, however, we used the logarithms of intensities and showed that this allows turbulence studies beyond the regime, at which fluctuations of intensity would be useful.

A similar approach, potentially, is applicable to the VCS for studies of emitted radiation in the presence of significant absorption. Indeed, the equation of the radiative transfer provides us in this case with

$$I_{\mathbf{X}}(v) = \frac{\epsilon}{\alpha} \left[1 - e^{-\alpha \rho_s(\mathbf{X}, v)} \right] , \quad (40)$$

where the first term is a constant, that can be subtracted. If this is done, the logarithm can be taken of the intensity. Potentially, this should allow VCS studies of emission lines where, otherwise, absorption distorts the statistics.

The difficulty of such an approach is the uncertainty of the base level of the signal. Taking logarithm is a non-linear operation that may distort the result, if the base level of signal is not accounted for properly. However, the advantage of the approach that potentially it allows studies of velocity turbulence, when the traditional VCA and VCS fail. Further research should clarify the utility of this approach.

4.2. Prospects of Studying ISM Turbulence with Absorption Lines

The study of turbulence using the modified VCS technique above should be reliable for optical depth τ up to 10^3 . For this range of optical depth, the line width is determined by Doppler shifts rather than the atomic constants. While formally the entire line profile provides information about the turbulence, in reality, the flat saturated part of the profile will contain only noise and will not be useful for any statistical study. Thus, the wings of the lines will contain signal.

As several absorption lines can be available along the same line of sight, this allows to extend the reliability of measurements combining them together. We believe that piecewise analyses of the wings belonging to different absorption lines is advantageous.

The actual data analysis may employ fitting the data with models, that, apart from the spectral index, specify the turbulence injection scale and velocity dispersion, as this is done in Chepurnov et al. (2006).

Note, that measurements of turbulence in the same volume using different absorption lines can provide complementary information. Formally, if lines with weak absorption, i.e. $\tau_0 < 1$ are available, there is no need for other measurements. However, in the presence of inevitable noise, the situation may be far from trivial. Naturally, noise of a constant level, e.g. instrumental noise, will affect more weak absorption lines. The strong absorption lines, in terms of VCS sample turbulence only for sufficiently large k_v . This limits the range of turbulent scales that can be sampled with the technique. However, the contrast that is obtained with the strong absorption lines is higher, which provides an opportunity of increasing signal to noise ratio for the range of k_v that is sampled by the absorption lines. If, however, a single strong absorption line is used, an analogy with a two dish radio interferometer is appropriate. Every dish of the radio interferometer samples spatial frequencies in the range approximately $[1/\lambda, 1/d]$, where λ is the operational wavelength, d is the diameter of the dish. In addition, the radio interferometer samples the spatial frequency $1/D$, where D is the distance between the dishes. Similarly, a strong absorption line provides with the information on turbulent velocity at the largest spatial scale of the emitting objects, as well as the fluctuation corresponding to the scales k_{window}, k_{abs} .

In LP06 we concentrated on obtaining asymptotic regimes for studying turbulence. At the same time in Chepurnov et al. (2006) fitting models of turbulence to the data was attempted. In the latter approach non-power law observed spectra can be used, which is advantageous for actual data, for which the range of scales in k_v is rather limited. Indeed, for HI with the injection velocities of 10 km/s and the thermal velocities of 1 km/s provides an order of magnitude of effective "inertial range". Correcting for thermal velocities one can increase this range by a factor, which depends on the signal to noise ratio of the data. Using heavier species rather than hydrogen one can increase the range by a factor $(m_{heavy}/m_H)^{1/2}$. This may or may not be enough for observing good asymptotics.

We have seen in ?? that for absorption lines the introduction of windows determined by the width of the line wings introduces additional distortions of the power spectrum. However, this is not a problem if, instead of asymptotics, fitting of the model is used. Compared to the models used in Chepurnov et al. (2006) the models for absorption lines should also have to model the window induced by the absorption. The advantage is, however, that absorption lines provide a pure pencil beam observations.

4.3. Comparison and synergy with other techniques

Formally, there exists an extensive list of different tools to study turbulence that predated our studies (see Lazarian 1999 and ref. therein). However, a closer examination shows that this list is not as impressive as it looks. Moreover, our research showed that some techniques may provide confusing, if not erroneous, output, unless theoretical understanding of what they measure is achieved. For instance, we mentioned in the introduction an example of the erroneous application of velocity centroids to supersonic molecular cloud data. Note, that clumps and shell finding algorithms would find a hierarchy of clumps/shells for synthetic observations obtained with *incompressible* simulations. This calls for a more cautious approach to the interpretation of the results of some of the accepted techniques.

For instance, the use of different wavelets for the analysis of data is frequently treated in the literature as different statistical techniques of turbulence studies (Gill & Henriksen 1990, Stutzki et al. 1998, Cambresy 1999, Khalil et al. 2006), which creates an illusion of an excessive wealth of tools and approaches. In reality, while Fourier transforms

use harmonics of $e^{i\mathbf{kr}}$, wavelets use more sophisticated basis functions, which may be more appropriate for problems at hand. In our studies we also use wavelets both to analyze the results of computations (see Kowal & Lazarian 2006a) and synthetic maps (Ossenkopf et al. 2006, Esquivel et al. 2007), along with or instead of Fourier transforms or correlation functions. Wavelets may reduce the noise arising from inhomogeneity of data, but we found in the situations when correlation functions of centroids that we studied were failing as the Mach number was increasing, a popular wavelet (Δ -variance) was also failing (cp. Esquivel & Lazarian 2005, Ossenkopf et al. 2006, Esquivel et al. 2007).

While in wavelets the basis functions are fixed, a more sophisticated technique, Principal Component Analysis (PCA), chooses basis functions that are, in some sense, the most descriptive. Nevertheless, the empirical relations obtained with PCA for extracting velocity statistics provide, according to Padoan et al. (2006), an uncertainty of the velocity spectral index of the order 0.5 (see also Brunt et al. 2003), which is too large for testing most of the turbulence theories. In addition, while our research in LP00 shows that for density spectra $E_\rho \sim k^{-\alpha}$, for $\alpha < 1$ both velocity and density fluctuations influence the statistics of PPV cubes, no dependencies of PPV statistics on density have been reported so far in PCA studies. This also may reflect the problem of finding the underlying relations empirically with data cubes of limited resolution. The latter provides a special kind of shot noise, which is discussed in a number of papers (Lazarian et al. 2001, Esquivel et al. 2003, Chepurnov & Lazarian 2006a).

Spectral Correlation Function (SCF) (see Rosolowsky et al. 1999 for its original form) is another way to study turbulence. Further development of the SCF technique in Padoan et al. (2001) removed the adjustable parameters from the original expression for the SCF and made the technique rather similar to VCA in terms of the observational data analysis. Indeed, both SCF and VCA measure correlations of intensity in PPV “slices” (channel maps with a given velocity window Δv), but if SCF treats the outcome empirically, the analytical relations in Lazarian & Pogosyan (2000) relate the VCA measures to the underlying velocity and density statistics. Mathematically, SCF contains additional square roots and normalizations compared to the VCA expressions. Those make the analytical treatment, which is possible for simpler VCA expressions, prohibitive. One might speculate that, similar to the case of conventional centroids and not normalized centroids introduced in Lazarian & Esquivel (2003), the actual difference between the statistics measured by the VCA and SCF is not significant.

In fact, we predicted several physically-motivated regimes for VCA studies. For instance, slices are “thick” for eddies with velocity ranges less than Δv and “thin” otherwise. VCA relates the spectral index of intensity fluctuations within channel maps to the thickness of the velocity channel and to the underlying velocity and density in the emitting turbulent volume⁷. In the VCA these variations of indexes with the thickness of PPV “slice” are used to disentangle velocity and density contributions. We suspect that similar “thick” and “thin” slice regimes should be present in the SCF analysis of data, but they have not been reported yet. While the VCA can be used for all the purposes the SCF is used (e.g. for an empirical comparisons of simulations and observations), the opposite is not true. In fact, Padoan et al. (2004) stressed that VCA eliminates errors inevitable for empirical attempts to calibrate PPV fluctuations in terms of the underlying 3D velocity spectrum.

VCS is a statistical tool that uses the information of fluctuations along the velocity axis of the PPV. Among all the tools that use spectral data, including the VCA, it is unique, as it *does not* require spatial resolution. This is why, dealing with the absorption lines, where good spatial coverage is problematic, we employed the VCS. Potentially, having many sources sampling the object one can create PPV cubes and also apply the VCA technique. However, this requires very extended data sets, while for the VCS sampling with 5 or 10 sources can be sufficient for obtaining good statistics (Chepurnov & Lazarian 2006a).

We feel that dealing with the ISM turbulence, it is synergetic to combine different approaches. For the wavelets used their relation with the underlying Fourier spectrum is usually well defined. Therefore the formulation of the theory (presented in this work, as well as, in our earlier papers in terms of the Fourier transforms) in terms of wavelets is straightforward. At the same time, the analysis of data with the wavelets may be advantageous, especially, in the situations when one has to deal with window functions.

5. SUMMARY

In the paper above we have shown that

- Studies of turbulence with absorption lines are possible with the VCS technique if, instead of intensity $I(\nu)$, one uses the logarithm of the absorbed intensity $\log I_{abs}(\nu)$, which is equivalent to the optical depth $\tau(\nu)$.
- In the weak absorption regime, i.e. when the optical depth at the middle of the absorption line is less than unity, the analysis of the $\tau(\nu)$ coincides with the analysis of intensities of emission for ideal resolution that we discussed in LP06.
- In the intermediate absorption regime, i.e. when the optical depth at the middle of the absorption line is larger than unity, but less than 10^3 , the wings of the absorption line can be used for the analysis. The saturated part of the line is expected to be noise dominated.
- The higher the absorption, the less the portion of the spectrum corresponds to the wings available for the

⁷ We showed that much of the earlier confusion stemmed from different observational groups having used velocity channels of different thicknesses (compare, e.g., Green 1993 and Stanimirovic et al. 1999).

analysis. In terms of the mathematical setting this introduces and additional window in the expressions for the VCS analysis. However, the contrast of the small scale fluctuations increases with the decrease of the window.

- For strong absorption regime, the broadening is determined by Lorentzian wings of the line and therefore no information on turbulence is available.

APPENDIX

DERIVATION OF THE POWER SPECTRUM P_τ

Following eqns. (20,21) the power spectrum of the optical depth is

$$P_\tau(k_v) = \alpha(\nu_0)^2 \int_0^S dz_1 \int_0^S dz_2 \xi(|z_1 - z_2|) \int_{-\infty}^{\infty} dk'_v \int_{-\infty}^{\infty} dk''_v \\ \times e^{-\frac{1}{2}k_v^{+2}D^-} e^{-\frac{1}{4}k_v^{-2}D^+} e^{-(|k'_v| + |k''_v|)a} W\left(k_v - k_v^+ - \frac{k_v^-}{2}\right) W^*\left(k_v - k_v^+ + \frac{k_v^-}{2}\right) \quad (\text{A1})$$

where $D^- = D_z(|z_1 - z_2|) + 2\beta$ and $D^+ = D_z(S) - D_z(|z_1 - z_2|)/2 + \beta$ while $k_v^+ = (k'_v + k''_v)/2$ and $k_v^- = k'_v - k''_v$. Since the mask is real, $W^*(k_v) = W(-k_v)$.

To deal with absolute values in the Lorentz transform, we split integration regions in quadrants I – ($k'_v > 0, k''_v > 0$), II – ($k'_v < 0, k''_v > 0$), III – ($k'_v < 0, k''_v < 0$) and IV – ($k'_v > 0, k''_v < 0$). Integration over quadrants III and IV can be folded into integration over regions I and II respectively by substitution $k'_v \rightarrow -k'_v, k''_v \rightarrow -k''_v, k_v^+ \rightarrow -k_v^+, k_v^- \rightarrow -k_v^-$. Writing out only integration over k_v

$$I + III: \int_0^\infty dk'_v \int_0^\infty dk''_v e^{-\frac{1}{2}k_v^{+2}D^-} e^{-\frac{1}{4}k_v^{-2}D^+} e^{-2ak_v^+} \\ \times \left[W\left(k_v - k_v^+ - \frac{k_v^-}{2}\right) W\left(k_v^+ - k_v - \frac{k_v^-}{2}\right) + W\left(k_v + k_v^+ + \frac{k_v^-}{2}\right) W\left(-k_v - k_v^+ + \frac{k_v^-}{2}\right) \right] \quad (\text{A2})$$

$$II + IV: \int_0^\infty dk'_v \int_{-\infty}^0 dk''_v e^{-\frac{1}{2}k_v^{+2}D^-} e^{-\frac{1}{4}k_v^{-2}D^+} e^{-ak_v^-} \\ \times \left[W\left(k_v - k_v^+ - \frac{k_v^-}{2}\right) W\left(k_v^+ - k_v - \frac{k_v^-}{2}\right) + W\left(k_v + k_v^+ + \frac{k_v^-}{2}\right) W\left(-k_v - k_v^+ + \frac{k_v^-}{2}\right) \right] \quad (\text{A3})$$

Changing variables of integration to k_v^+ and k_v^-

$$I + III: \int_0^\infty dk_v^+ e^{-\frac{1}{2}k_v^{+2}D^-} e^{-2ak_v^+} \int_{-2k_v^+}^{2k_v^+} dk_v^- e^{-\frac{1}{4}k_v^{-2}D^+} \\ \times \left[W\left(k_v - k_v^+ - \frac{k_v^-}{2}\right) W\left(k_v^+ - k_v - \frac{k_v^-}{2}\right) + W\left(k_v + k_v^+ + \frac{k_v^-}{2}\right) W\left(-k_v - k_v^+ + \frac{k_v^-}{2}\right) \right] \quad (\text{A4})$$

$$II + IV: \int_{-\infty}^\infty dk_v^+ e^{-\frac{1}{2}k_v^{+2}D^-} \int_{|2k_v^+|}^\infty dk_v^- e^{-\frac{1}{4}k_v^{-2}D^+} e^{-ak_v^-} \\ \times \left[W\left(k_v - k_v^+ - \frac{k_v^-}{2}\right) W\left(k_v^+ - k_v - \frac{k_v^-}{2}\right) + W\left(k_v + k_v^+ + \frac{k_v^-}{2}\right) W\left(-k_v - k_v^+ + \frac{k_v^-}{2}\right) \right] \quad (\text{A5})$$

At the end, the integrals can be combined into the main contribution and the correction that manifests itself only when Lorentz broadening is significant.

$$\text{main: } \int_0^\infty dk_v^+ e^{-\frac{1}{2}k_v^{+2}D^-} e^{-2ak_v^+} \int_0^\infty dk_v^- e^{-\frac{1}{4}k_v^{-2}D^+} \tilde{W}(k_v, k_v^+, k_v^-) \quad (\text{A6})$$

$$\text{corr } \int_0^\infty dk_v^+ e^{-\frac{1}{2}k_v^{+2}D^-} \int_{2k_v^+}^\infty dk_v^- e^{-\frac{1}{4}k_v^{-2}D^+} \left(e^{-ak_v^-} - e^{-2ak_v^+} \right) \tilde{W}(k_v, k_v^+, k_v^-) \quad (\text{A7})$$

where symmetrized window is

$$\begin{aligned} \tilde{W}(k_v, k_v^+, k_v^-) \equiv & \\ & W\left(k_v - k_v^+ - \frac{k_v^-}{2}\right) W\left(k_v^+ - k_v - \frac{k_v^-}{2}\right) + W\left(k_v + k_v^+ + \frac{k_v^-}{2}\right) W\left(-k_v - k_v^+ + \frac{k_v^-}{2}\right) + \\ & W\left(k_v - k_v^+ - \frac{k_v^-}{2}\right) W\left(k_v^+ - k_v - \frac{k_v^-}{2}\right) + W\left(k_v + k_v^+ + \frac{k_v^-}{2}\right) W\left(-k_v - k_v^+ + \frac{k_v^-}{2}\right) \end{aligned} \quad (\text{A8})$$

The final expression for $P_\tau(k_v)$ is then

$$\begin{aligned} P_\tau(k_v) = & \alpha^2 S \int_0^S dz (S - |z|) \xi(z) \int_0^\infty dk_v^+ e^{-2k_v^+ a} e^{-\frac{1}{2} k_v^{+2} D^-} \int_0^\infty dk_v^- e^{-\frac{1}{4} k_v^{-2} D^+} \tilde{W} \\ & + \alpha^2 S \int_0^S dz (S - |z|) \xi(z) \int_0^\infty dk_v^+ e^{-\frac{1}{2} k_v^{+2} D^-} \int_{2k_v^+}^\infty dk_v^- e^{-\frac{1}{4} k_v^{-2} D^+} \left(e^{-k_v^- a} - e^{-2k_v^+ a} \right) \tilde{W} \end{aligned} \quad (\text{A9})$$

REFERENCES

Armstrong, J. W., Rickett, B. J., & Spangler, S. R. 1995, ApJ, 443, 209

Ballesteros-Paredes, J., Klessen, R., Mac Low, M. & Vasquez-Semadeni, E. 2006, in "Protostars and Planets V", Reipurth, D. Jewitt, and K. Keil (eds.), University of Arizona Press, Tucson, 951 pp., 2007., p.63-80

Beresnyak, A. & Lazarian, A., ApJL, 640, L175

Beresnyak, A., Lazarian, A., Cho, J. 2005, ApJ, 624, L93

Biskamp, D. 2003, Magnetohydrodynamical Turbulence (Cambridge, CUP)

Brunt, C.M., Heyer, M.H., Vazquez-Semadeni, E., & Pichardo, B. 2003, ApJ, 595, 824-84

Cambresy, L. 1999, A&A, 345, 965

Chepurnov, A. & Lazarian, A. 2006a, astro-ph/0611463

Chepurnov, A. & Lazarian, A. 2006b, astro-ph/0611465

Chepurnov, A., Lazarian, A., Stanićirović, S., Peek, J., & Heiles, C. 2006, astro-ph/0611462

Cho, J., & Lazarian, A. 2003, MNRAS, 345, 325

Cho, J., & Lazarian, A. 2004, ApJ, 615, L41

Cho, J., & Lazarian, A. 2005, Theoretical and Computational Fluid Dynamics, 19, 127

Cho, J., Lazarian, A., Honein, A., Knaepen, B., Kassinos, S., & Moin, P. 2003, ApJ, 589, L77

Deshpande, A.A. 2000, MNRAS, 317, 199

Deshpande, A.A., Dwarakanath, K.S., Goss, W.M., 2000, ApJ, 543, 227

Dickman, R. L., & Kleiner, S. C. 1985, ApJ, 295, 479

Elmegreen, B. 2002, ApJ, 577, 206

Elmegreen, B. & Falgarone, E. 1996, ApJ, 471, 816

Elmegreen, B. & Scalo, J. 2004, ARA&A, 42, 211

Esquivel, A. & Lazarian, A. 2005, ApJ, 631, 320

Esquivel, A., Lazarian, A., Horibe, S., Ossenkopf, V., Stutzki, J., Cho, J. 2007, MNRAS, 381, 1733

Esquivel, A., Lazarian, A., Pogosyan, D., & Cho, J. 2003, MNRAS, 342, 325

Falgarone, E. 1999, in *Interstellar Turbulence*, ed. by J. Franco, A. Carraminana, CUP, (henceforth *Interstellar Turbulence*) p.132

Gill, A. & Henriksen, R.N. 1990, ApJ, 365, L27

Heiles, C. & Troland, T.H. 2004, ApJS, 151, 271

Heyer, M. & Brunt, C. 2004, ApJ, 615, 45

Inogamov, N.A. & Sunyaev, R.A. 2003, Astronomy Letters, 29, 791

Khalil, A., Joncas, G., Nekka, F., Kestener, P., & Arneodo, A. 2006, ApJS, 165, 512-550

Kim, J., & Ryu, D. 2005, ApJ, 630, L45

Kleiner, S. C., & Dickman, R. L. 1985, ApJ, 295, 466

Lazarian, A. 1995, A& A, 293, 507

Lazarian, A. 1999, in *Plasma Turbulence and Energetic Particles in Astrophysics*, Eds. Michal Ostrowski and Reinhard Schlickeiser, Cracow, 28-47

Lazarian, A. 2004, Journal of Korean Astronomical Society, 37, 563

Lazarian, A. 2005, BAAS, 207, 119.02

Lazarian, A. 2006, Astron. Nachricht., 609, issue 5/6, 327

Lazarian, A. & Esquivel, E. 2003, ApJ, 592, L37

Lazarian, A., & Pogosyan, D. 2000, ApJ, 537, 72

Lazarian, A., & Pogosyan, D. 2004, ApJ, 616, 943

Lazarian, A. & Pogosyan, D. 2006, ApJ, 652, 1348-1366

Lazarian, A., Pogosyan, D., & Esquivel, A. 2002, in ASP Conf. Ser. 276, Seeing Through the Dust, ed. R. Taylor, T. L. Landecker, & A. G. Willis (San Francisco: ASP), 182

Lazarian, A., Pogosyan, D., Vázquez-Semadeni, E., & Pichardo, B. 2001, ApJ, 555, 130

Lazarian, A., Vishwanic, E., Cho, J. 2004, ApJ, 603, 180

Lazarian, A. & Yan, H. 2004, in "Astrophysical Dust" eds. A. Witt & B. Draine, APS, V. 309, p.479

Maron, J. & Goldreich, P. 2001, ApJ, 554, 1175

Mac Low, M.-M. & Klessen, R.S. 2004, *Reviews of Modern Physics*, 76, 125

McKee, Christopher F.; Tan, Jonathan C. 2002, Nature, 416, 59

McKee, C. & Ostriker, E. 2007, Theory of Star Formation, ARA&A, 45, 565-687

Monin, A.S. & Yaglom, A. M. 1975, Statistical Fluid Mechanics: Mechanics of Turbulence, Vol. 2 (Cambridge: MIT Press)

Munch, G. 1999, in "Interstellar Turbulence", eds. J. Franco and A. Carraminana, CUP, p. 1

Munch, G. 1958, Rev. Mod. Phys., 30, 1035

Narayan, R., & Goodman, J. 1989, MNRAS, 238, 963

Ossenkopf, V., Esquivel, A., Lazarian, A. & Stutzki, J. 2005, A&A, 452, 223-236

O'Dell C.R. & Casteneda, H., 1987, ApJ, 317, 686

Rosolowsky, E.W. Goodman, A. A.; Wilner, D. J.; Williams, J. P. 1999, ApJ, 524, 887

Padoan, P., Goodman, A.A., & Javala, M. 2003, ApJ, 588, 881

Padoan, P., Jimenez, R., Juvela, M. & Norlund, A. 2004, ApJ, L49

Padoan, P., Rosolowsky, E. W., & Goodman, A. A. 2001, ApJ, 547, 862

Padoan, P., Juvela, M., Kritsuk, A. & Norman, M. 2006, ApJ, 653, L125

Pudritz, R. E. 2001, From Darkness to Light: Origin and Evolution of Young Stellar Clusters, ASP , Vol. 243. Eds T. Montmerle and P. Andre. San Francisco, p.3

Spangler, S.R., & Gwinn, C.R. 1990, ApJ, 353, L29

Spitzer, L. 1978, Physical Processes in the Interstellar Medium, Wiley-Interscience, New York

Stanićirović, S., & Lazarian, A., 2001, ApJ, 551, 53

Stutzki, J. 2001, Astrophysics and Space Science Supplement, 277, 39

Sunyaev, R.A., Norman, M.L., & Bryan, G.L. 2003, Astronomy Letters, 29, 783

von Hoerner, S. 1951, Zeitschrift für Astrophysics, 30, 17

Wilson, O.C., Munch, G., Flather, E.M., & Coffeen, M.F. 1959, ApJS, 4, 199

Vázquez-Semadeni, E., Ostriker, E.C., Passot, T., Gammie, C.F., Stone, J.M. 2000, in *Protostars and Planets IV*, Tucson: University of Arisona Press, p. 3